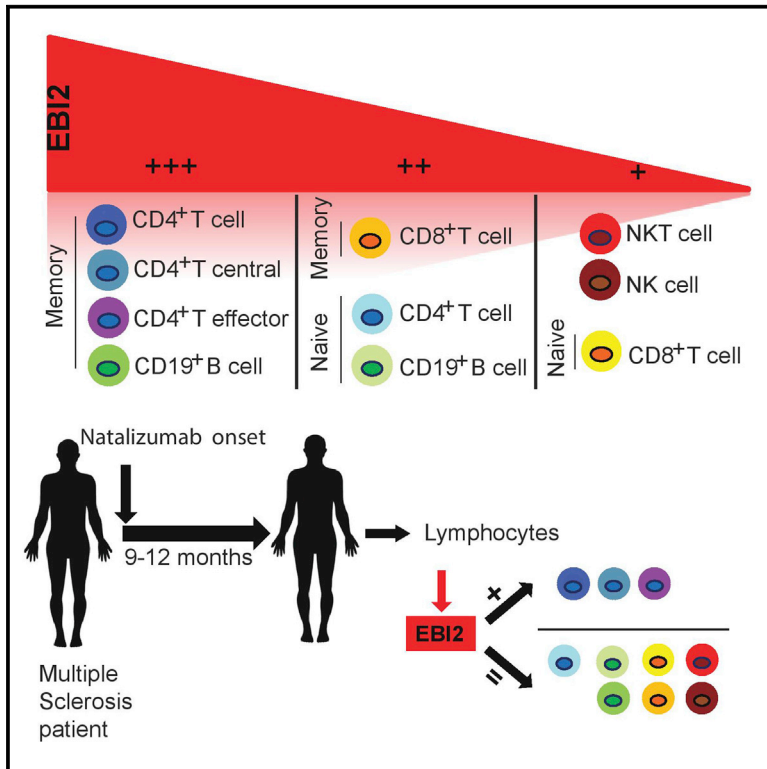


## EBI2 Expression and Function: Robust in Memory Lymphocytes and Increased by Natalizumab in Multiple Sclerosis

### Graphical Abstract



### Authors

Aurélie S. Clottu, Amandine Mathias, Andreas W. Sailer, Myriam Schlupe, Jörg D. Seebach, Renaud Du Pasquier, Caroline Pot

### Correspondence

caroline.pot-kreis@chuv.ch

### In Brief

Clottu et al. investigated the expression and function of the oxysterol receptor EBI2 in human primary lymphocytes. They show that EBI2 regulates human lymphocyte migration in vitro and that its expression and migratory response are increased in memory CD4<sup>+</sup> T cells from multiple sclerosis patients treated with natalizumab.

### Highlights

- EBI2 expression is maximal on human CD4<sup>+</sup> T cells and CD19<sup>+</sup> B cells
- EBI2 is functional in human T and B cells
- Natalizumab alters EBI2 expression and function in memory CD4<sup>+</sup> T cells



# EBI2 Expression and Function: Robust in Memory Lymphocytes and Increased by Natalizumab in Multiple Sclerosis

Aurélie S. Clottu,<sup>1,2,3</sup> Amandine Mathias,<sup>1</sup> Andreas W. Sailer,<sup>4</sup> Myriam Schlupe,<sup>5</sup> Jörg D. Seebach,<sup>3</sup> Renaud Du Pasquier,<sup>1,5</sup> and Caroline Pot<sup>1,2,5,6,\*</sup>

<sup>1</sup>Laboratories of Neuroimmunology, Neuroscience Research Center, Department of Clinical Neurosciences, Lausanne University Hospital, Chemin des Boveresses 155, 1066 Epalinges, Switzerland

<sup>2</sup>Department of Pathology and Immunology, Geneva University Medical Center, Rue Michel-Servet 1, 1211 Geneva 4, Switzerland

<sup>3</sup>Division of Immunology and Allergology, Department of Medical Specialties, Geneva University Hospitals, Rue Gabrielle-Perret-Gentil 4, 1211 Geneva 14, Switzerland

<sup>4</sup>Developmental and Molecular Pathways, Novartis Institutes for BioMedical Research, Forum 1, 4002 Basel, Switzerland

<sup>5</sup>Division of Neurology, Department of Clinical Neurosciences, Lausanne University Hospital, Rue du Bugnon 46, 1011 Lausanne, Switzerland

<sup>6</sup>Lead Contact

\*Correspondence: [caroline.pot-kreis@chuv.ch](mailto:caroline.pot-kreis@chuv.ch)  
<http://dx.doi.org/10.1016/j.celrep.2016.12.006>

## SUMMARY

The interaction between oxysterols and the G protein-coupled receptor Epstein-Barr virus-induced gene 2 (EBI2) fine-tunes immune cell migration, a mechanism efficiently targeted by several disease-modifying treatments developed to treat multiple sclerosis (MS), such as natalizumab. We previously showed that memory CD4<sup>+</sup> T lymphocytes migrate specifically in response to 7 $\alpha$ ,25-dihydroxycholesterol (7 $\alpha$ ,25-OHC) via EBI2 in the MS murine model experimental autoimmune encephalomyelitis. However, the EBI2 expression profile in human lymphocytes in both healthy and MS donors is unknown. Here, we characterize EBI2 biology in human lymphocytes. We observed that EBI2 is functionally expressed on memory CD4<sup>+</sup> T cells and is enhanced under natalizumab treatment. These data suggest a significant role for EBI2 in human CD4<sup>+</sup> T cell migration, notably in patients with MS. Better knowledge of EBI2 involvement in autoimmunity may therefore lead to an improved understanding of the physiopathology of MS.

## INTRODUCTION

Multiple sclerosis (MS) is a frequent chronic inflammatory disease of the CNS leading to neurologic disability and lifelong morbidity in young adults (Compston and Coles, 2002). Despite advances in MS research, its pathophysiology is still far from being well understood, so it remains an incurable disease. In addition, many patients still do not respond appropriately to available drugs or experience heavy side effects. Inflammation in MS involves circulating auto-reactive T cells, which escape immune regulation and enter the brain, resulting in inflammatory infiltrates

and demyelination throughout the CNS (Compston and Coles, 2002). Thus, immune cell migration is a key point in the disease process (Engelhardt and Ransohoff, 2012). Subsets of oxidized cholesterol metabolites, oxysterols, were reported to play a role in inflammation and immune cell chemotaxis (Bauman et al., 2009; Yi et al., 2012). More precisely, the oxysterol 7 $\alpha$ ,25-dihydroxycholesterol (7 $\alpha$ ,25-OHC), synthesized through the enzymes cholesterol 25-hydroxylase and 25-hydroxycholesterol 7- $\alpha$ -hydroxylase, was characterized as having peculiar chemotactic properties by being the strongest ligand activating the Epstein-Barr virus-induced gene 2 (EBI2) receptor (Hanedouche et al., 2011; Liu et al., 2011). The expression of this receptor is well characterized on murine immune cells and found to be maximal on mature B cells and CD4<sup>+</sup> T cells, including T follicular helper (Tfh) cells, but is also described on dendritic cells (DC) and plasmacytoid DCs (pDCs) (Chiang et al., 2013; Gatto et al., 2013; Li et al., 2016; Pereira et al., 2009; Suan et al., 2015). In vivo, EBI2 activation was reported to direct B and Tfh cell positioning in follicles and osteoclasts migration toward bone surface (Gatto et al., 2009; Kelly et al., 2011; Li et al., 2016; Nevius et al., 2015; Pereira et al., 2009; Suan et al., 2015; Yi et al., 2012). We showed that EBI2 promoted memory CD44<sup>+</sup>CD4<sup>+</sup> T cell, particularly interleukin (IL)-17-secreting T cell, and migration during experimental autoimmune encephalomyelitis (EAE) (Chalmin et al., 2015). In human, EBI2 is further expressed and promotes the in vitro migration of astrocytes and macrophages (Eibinger et al., 2013; Preuss et al., 2014; Rutkowska et al., 2015). However, the expression and the function of EBI2 in human lymphocytes are scarcely studied, while EBI2's potential role in MS and the impact of disease-modifying treatments (DMTs) on this receptor biology have not been examined. In this study, we aimed to characterize the expression and function of EBI2 in human peripheral blood lymphocytes by using flow cytometry and an in vitro migration assay. We tested lymphocytes obtained from healthy donors (HDs) and relapsing-remitting multiple sclerosis (RRMS) patients who were either untreated or receiving a DMT, in particular natalizumab, a

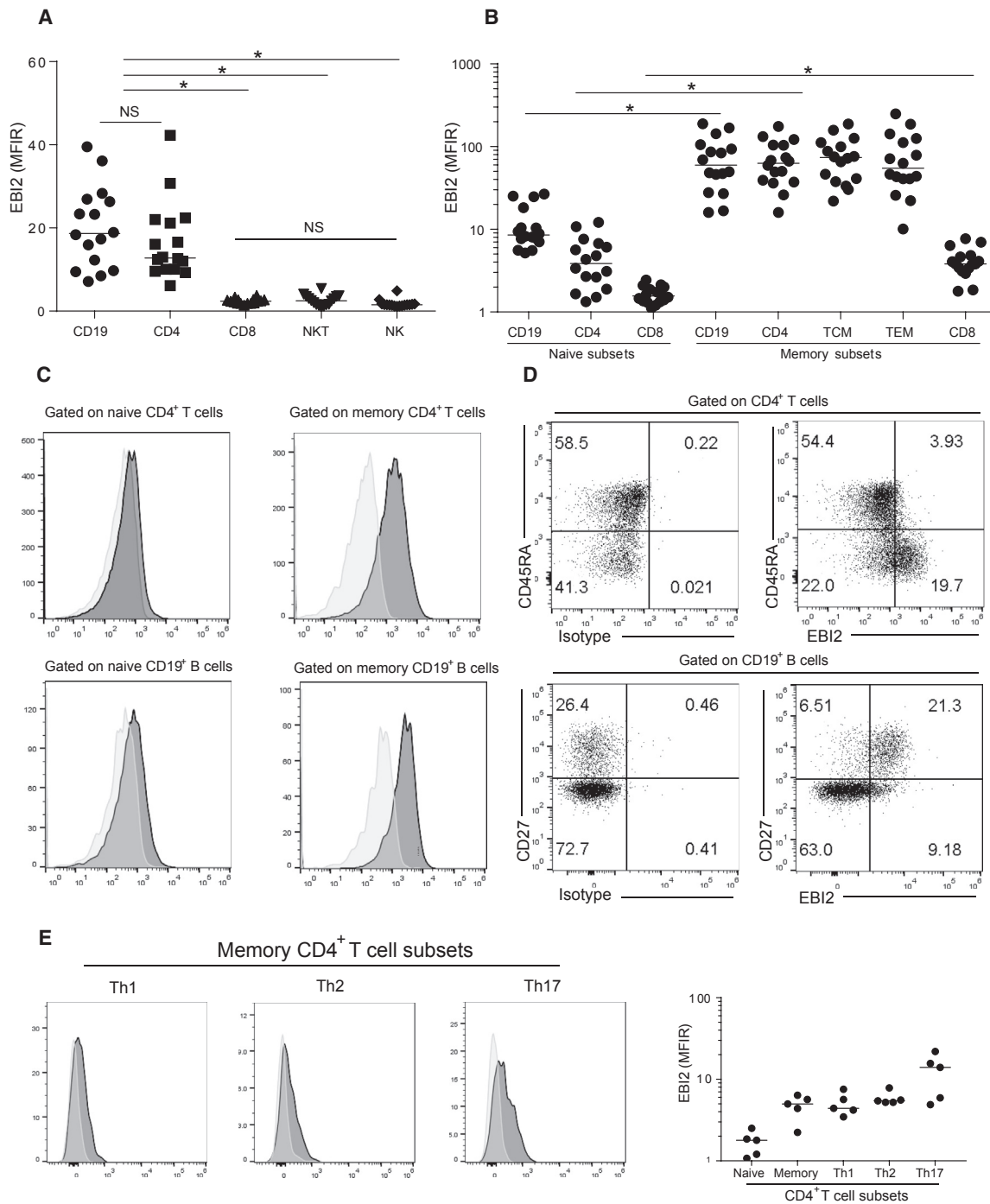


**Figure 1. EB12 Expression in Human Lymphocytes from HDs**

Cryopreserved human peripheral blood mononuclear cells (PBMCs) were analyzed by flow cytometry.

(A) EB12 expression shown as mean fluorescence intensity ratios (MFIRs) in total CD19<sup>+</sup> B, CD4<sup>+</sup> T, CD8<sup>+</sup> T, NKT (CD3<sup>+</sup>CD56<sup>+</sup>), and NK (CD3<sup>-</sup>CD56<sup>+</sup>) cells, gated after dead cells and doublet exclusion.

(B) EB12 MFIRs in naive (CD19<sup>+</sup>CD27<sup>-</sup>) and memory (CD19<sup>+</sup>CD27<sup>+</sup>) subsets of B cells and in naive (CD45RA<sup>+</sup>) and memory (CD45RA<sup>-</sup>) CD4<sup>+</sup> and CD8<sup>+</sup> T cells, with CD4<sup>+</sup> T cell effector memory (TEM, CCR7<sup>-</sup>) and central memory (TCM, CCR7<sup>+</sup>) subtypes.

(C) Fluorescence histograms showing EB12 (dark gray) and isotype (light gray) in naive versus memory subsets of CD4<sup>+</sup> T cells (upper panels) and CD19<sup>+</sup> B cells (lower panels).

(D) Comparison between isotype (left) or EB12 (right) stainings in CD4<sup>+</sup> T cells (upper) or B cells (lower). Numbers in each quadrant indicate the percentage of cells.

(legend continued on next page)

humanized monoclonal immunoglobulin G4 (IgG4) (Börnsen et al., 2012) antibody blocking the  $\alpha_4$ -integrin subunit and thus interfering with leukocytes migration to the CNS (Engelhardt and Kappos, 2008).

## RESULTS

### EBI2 Is Highly Expressed on Human Memory Lymphocytes

To characterize the role of EBI2 in human lymphocytes, we first analyzed its expression by flow cytometry on different subsets of human peripheral blood mononuclear cells (PBMCs) from HDs using a specific anti-EBI2 antibody (clone 57C9B5C9) (Rutkowska et al., 2015) or the corresponding isotype. EBI2 was detected at the highest level in CD19<sup>+</sup> B cells and CD4<sup>+</sup> T cells with an average of mean fluorescence intensity ratios (MFIRs) 20 times higher compared to CD8<sup>+</sup> T, natural killer T (NKT), and NK cells that showed low EBI2 expression (Figures 1A and S1A). Using the EAE model, we previously reported that CD4<sup>+</sup>CD44<sup>+</sup> memory lymphocytes depicted higher EBI2 expression and migration toward 7 $\alpha$ ,25-OHC compared to their naive correlates (Chalmin et al., 2015). Therefore, we here asked whether memory versus naive lymphocyte subsets would differentially express EBI2 in the human setting as well. The highest EBI2 expression was detected in memory subsets of lymphocytes, with memory T (CD45RA<sup>-</sup>CD4<sup>+</sup>) and B (CD27<sup>+</sup>CD19<sup>+</sup>) cells expressing significantly more EBI2 compared to their naive counterparts (Figures 1B and S1A). In the B cell subset, CD27 is also co-expressed with CD19<sup>+</sup> on plasmablasts that do not express the CD20 marker. However, a contribution of plasmablasts to EBI2 expression is unlikely, because we did not detect a significant amount of CD19<sup>+</sup>CD20<sup>-</sup> B cells in our samples (data not shown). Memory CD4<sup>+</sup> T cells can be further divided into two memory pools, the T central memory (TCM) and T effector memory (TEM) subsets, that have distinct homing potentials and are characterized by a different expression of C-C chemokine receptor 7 (CCR7) (Sallusto et al., 1999). Some subsets of integrins and chemokine or sphingosine receptors implicated in leukocyte trafficking have been shown to have distinct actions on these two subsets (Mehling et al., 2008; Sallusto et al., 1999). We therefore wondered whether EBI2 expression could diverge in the latter populations, but we detected similar EBI2 expression levels between them (Figures 1B and S1A). Memory CD45RA<sup>-</sup>CD8<sup>+</sup> T cells also depicted higher EBI2 expression compared to naive subsets, although at very low levels compared to B and CD4<sup>+</sup> T cells (Figure 1B).

We further questioned whether the entire versus parts of the memory cell population expressed EBI2. Compared to the isotype, the EBI2 staining revealed a predominant fluorescence shift in the memory subsets of CD4<sup>+</sup> T and CD19<sup>+</sup> B cells (Figures 1C and S1A) associated to a deviation of the entire memory but not of the naive populations, without the apparition of a distinct

subpopulation neither in the CD19<sup>+</sup> B nor in the CD4<sup>+</sup> T cell subsets (Figures 1D and S1A).

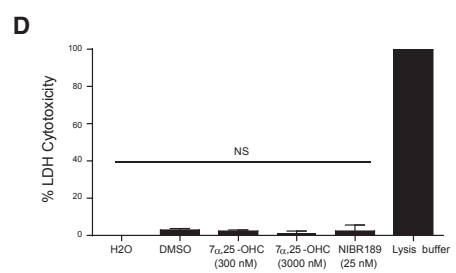
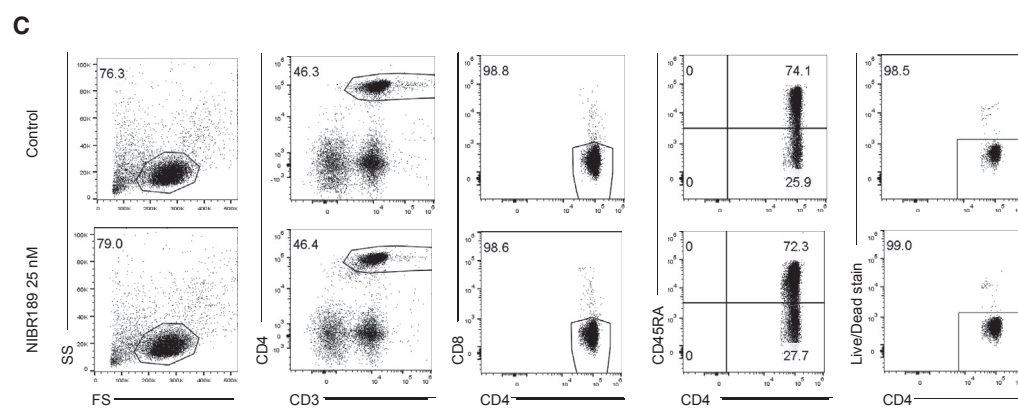
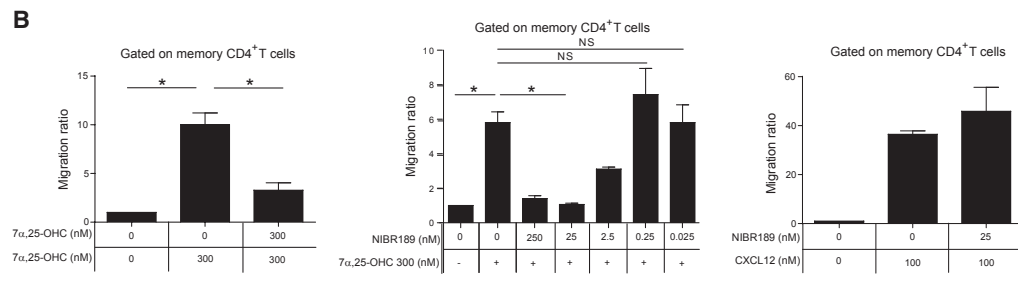
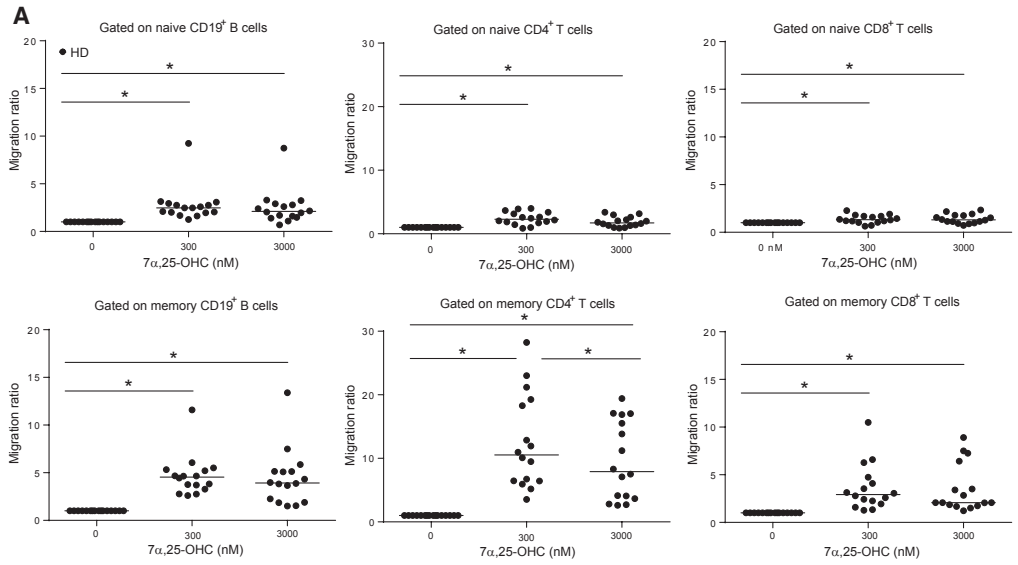
We next examined whether EBI2 would be differentially expressed in differentiated subsets of CD4<sup>+</sup> T helper cells, because we had previously shown using the murine EAE model that Th17 cells migrated maximally toward 7 $\alpha$ ,25-OHC and probably expressed EBI2 at a higher level compared to other CD4<sup>+</sup> T cell subsets. We therefore looked at ex vivo EBI2 expression on Th1, Th2, and Th17 memory subtypes defined using chemokine receptor surface markers (Th1, CXCR3<sup>+</sup>CCR4<sup>-</sup>; Th2, CXCR3<sup>-</sup>CCR4<sup>+</sup>; and Th17, CXCR3<sup>-</sup>CCR6<sup>+</sup>). Although Th17 cells showed a slightly increased shift in EBI2 expression compared to Th1 or Th2 subsets, no statistical difference in MFIRs was observed between them (Figures 1E and S1B).

### Migration toward 7 $\alpha$ ,25-OHC Is Maximal in Memory CD4<sup>+</sup> T Cells and EBI2 Dependent

To investigate whether EBI2 was functional and could promote lymphocyte trafficking, we tested the migration response of human whole PBMCs toward different concentrations of 7 $\alpha$ ,25-OHC in a transwell assay as previously described for murine lymphocytes (Chalmin et al., 2015). In our model, migration was highest at 300 nM, particularly in the memory CD4<sup>+</sup> T cells, with a concentration effect between 300 nM (mean 13.4  $\pm$  SD 7.5) and 3,000 nM (8.4  $\pm$  5.5). Consistent with EBI2 expression profiles, the migration was maximal in lymphocyte memory subsets (Figure 2A, lower panels), with a response five times higher at the concentration of 300 nM in memory CD4<sup>+</sup> T cells (13.4  $\pm$  7.5) compared to naive (2.4  $\pm$  1) (Figure 2A, upper panels). Memory B cells showed half-lower migration compared to memory CD4<sup>+</sup> T cells, while CD8<sup>+</sup> T cells migrated at the lowest level. Furthermore, we confirmed that the migration was EBI2 dependent in our model. Because such directed migration involves a gradient of EBI2 ligand, here 7 $\alpha$ ,25-OHC, we disrupted the gradient by adding the same amount of 7 $\alpha$ ,25-OHC in both the upper and the lower chambers. Abolishment of the gradient significantly decreased memory CD4<sup>+</sup> T cell migration (Figure 2B, left panel). We further inhibited the EBI2 receptor using a chemical compound, NIBR189, previously characterized to selectively inhibit this receptor (Gessier et al., 2014). NIBR189 dramatically diminished the migration of memory CD4<sup>+</sup> T cells in a concentration-dependent manner when added with the PBMCs in the transwell migration assay; the most efficient concentration in our model was determined to be 25 nM (Figure 2B, middle panel). To compare EBI2-dependent migration to a known lymphocyte chemoattractant, we used CXCL12 (SDF-1) (Liu and Dorovini-Zis, 2009) in our assay and found that the migration of memory CD4<sup>+</sup> T cells toward this agent was three times higher than the response obtained with 7 $\alpha$ ,25-OHC. In contrast, migration in response to CXCL12 was not affected by NIBR189 addition (Figure 2B, right panel). NIBR189 did not change cell viability (Figure 2C) or induced toxicity in lymphocytes (Figure 2D).

(E) Left: fluorescence histograms showing EBI2 (dark gray) and isotype (light gray) in Th1 (CXCR3<sup>+</sup>CCR4<sup>-</sup>), Th2 (CXCR3<sup>-</sup>CCR4<sup>+</sup>), and Th17 (CXCR3<sup>-</sup>CCR6<sup>+</sup>). Right: EBI2 MFIRs in naive and memory CD4<sup>+</sup> T cells, and Th1, Th2, and Th17 subsets (n = 5).

Statistics using two-way ANOVA with a Tukey's post hoc analysis or unpaired Student's t test, with a p value  $\leq$  0.05 considered significant (\*). Error bars represent median. See also Figure S1.



(legend on next page)

### EBI2 Is Functionally Expressed in MS Patients with a Distinct EBI2 Expression to Migration Correlation Pattern

After the characterization of EBI2 in HDs, we proposed to assess its role in a disease setting, i.e., in RRMS patients (characteristics detailed in Table 1), because we had previously shown that EBI2 affects memory CD4<sup>+</sup> T cell migration to the CNS during EAE (Chalmin et al., 2015). We first tested untreated RRMS patients experiencing a relapse at the time of blood drawing. The relapses were characterized by non-invalidating symptoms, and the patients were not treated with corticosteroids. The detected EBI2 expression levels in CD19<sup>+</sup> B cell, CD4<sup>+</sup> T cell, and CD8<sup>+</sup> T cell subsets from these RRMS patients was similar to HDs, but the data repartition showed a higher variability, especially in memory CD4<sup>+</sup> T cells (HD: 72.4 (±45) versus RRMS: 86.1 (±108)) (Figure 3A). The migration response to 7 $\alpha$ ,25-OHC was also maximal in all memory subsets, and reached the same levels as in HDs, with average migration ratios in memory CD4<sup>+</sup> T cells of 12 (±7) and 11 (±7) in HDs and RRMS patients, respectively, and a concentration effect from 7 $\alpha$ ,25-OHC 300 to 3,000 nM both in HDs (25% decrease of the median of migration ratios) and in RRMS patients (38% decrease of median) (Figure 3B). We further evaluated the correlation between EBI2 expression and migration toward 7 $\alpha$ ,25-OHC. Although we observed no correlation in all subsets of lymphocytes from HDs (Figure 3C, upper panels), in RRMS patients, we detected a positive correlation reaching statistical significance in memory CD8<sup>+</sup> T cells ( $p = 0.0143$ ) and a positive trend in memory CD4<sup>+</sup> T cells ( $p = 0.0885$ ) (Figure 3C, lower panels).

### Natalizumab Treatment Increases EBI2 Expression and Promotes Migration toward 7 $\alpha$ ,25-OHC in Memory CD4<sup>+</sup> T Cells

Natalizumab (NTZ) is a humanized monoclonal IgG4 antibody blocking the  $\alpha_4$ -integrin subunit (Börnsen et al., 2012; Engelhardt and Kappos, 2008). The latter associates in a heterodimer with  $\beta_1$  to form an adhesion molecule also called very late antigen-4 (VLA-4), which is required for immune cell migration to the brain by interacting with its main ligands: vascular-cell adhesion molecule 1 (VCAM-1) and fibronectin. VCAM-1 is expressed on CNS vessel endothelial cells and is upregulated during neuroinflammation (Engelhardt and Kappos, 2008). Other integrin ligands, such as intercellular adhesion molecule (ICAM)-1 and ICAM-2,

which bind  $\alpha_L\beta_2$  (CD11a/CD18), also called leukocyte function-associated antigen-1 (LFA-1) on T cells, are upregulated upon CNS inflammation (Engelhardt and Ransohoff, 2012). The major effect of NTZ is to strongly inhibit the migration of immune cells to the brain, and is used in clinics with a significant beneficial effect to prevent relapses and possibly progression of disability in patients with RRMS (Polman et al., 2006).

Because NTZ has been shown to alter cell surface molecules expression, such as LFA-1, we hypothesized that EBI2 expression and/or function may be changed upon NTZ treatment as well (Jilek et al., 2014). Therefore, we assessed EBI2 expression by flow cytometry and performed transwell assay as described earlier to analyze samples from RRMS patients before (T0) and after 9–12 months (T9–T12) of NTZ treatment (patient characteristics detailed on Table 1). We first confirmed that in this patient population, EBI2 expression was predominant in the memory subsets of CD4<sup>+</sup> and CD8<sup>+</sup> T cells and of B cells both at T0 and at T9–T12. However, EBI2 expression increased specifically in all memory CD4<sup>+</sup> T cell populations (total, central, and effector memory), with MFIRs increasing as much as three times under NTZ treatment. No consistent MFIR change was detected in the CD8<sup>+</sup> T cell or the CD19<sup>+</sup> B cell subsets at T9–T12 compared to T0 (Figure 4A). Because NTZ treatment is prescribed in patients experiencing aggressive disease courses, we wanted to determine whether the increase in EBI2 expression could be related to disease duration or disease severity, rather than to the treatment. EBI2 expression showed a correlation with neither disease evolution nor disease severity, expressed by the expanded disability status scale (EDSS) (Figure S2A). We further checked whether changes in EBI2 expression could be induced by another DMT. We thus analyzed samples from patients before (T0) and after 9–12 months (T9–T12) of dimethyl fumarate (DMF) treatment. We did not observe any significant changes in EBI2 expression under this drug (Figure S2B and Table S1).

We then assessed whether NTZ could enhance EBI2 function. When looking at the migration of paired samples at two time points of NTZ treatment, we noticed again a predominant response in all memory subsets, and consistent with EBI2 expression, an increase of migration at T9–T12 was seen only in memory CD4<sup>+</sup> T cells (Figure 4B). We further examined whether NIBR189 was sufficient to block EBI2-induced migration of NTZ-treated patient memory CD4<sup>+</sup> T cells and thus performed in vitro migration assay with NTZ patient PBMCs at

### Figure 2. Human Memory Lymphocytes from HDs Migrate toward 7 $\alpha$ ,25-OHC in an EBI2-Dependent Way In Vitro

HD PBMC migration was assessed by transwell assay and quantified by flow cytometry using flow count beads. The migration ratio corresponds to the number of cells migrating to a given condition divided by the number of cells migrating to medium only (concentration 0 nM).

(A) Migration in response to 7 $\alpha$ ,25-OHC (0, 300, and 3,000 nM) of CD19<sup>+</sup> B cells, CD4<sup>+</sup> T cells, and CD8<sup>+</sup> T cells in naive (upper panels) compared to memory (lower panels) subsets ( $n = 16$ ).

(B) Left: migration toward 7 $\alpha$ ,25-OHC (0 or 300 nM) of memory CD4<sup>+</sup> T cells without or with addition of 7 $\alpha$ ,25-OHC to the cells ( $n = 4$ ). Middle: migration of memory CD4<sup>+</sup> T cells toward 7 $\alpha$ ,25-OHC (0 or 300 nM) with or without different concentrations of NIBR189 ( $n = 2$ ). Right: migration of memory CD4<sup>+</sup> T cells toward CXCL12 (0 or 100 ng/mL) with or without NIBR189 ( $n = 2$ ) (25 nM).

(C) Human PBMCs were kept in culture medium for 3 hr at 37°C either with only culture medium or with additional NIBR189 (25 nM), stained for viability, and analyzed by flow cytometry. Numbers in quadrants indicate the percentage of cells. FS, forward scatter; SS, side scatter.

(D) Human PBMCs were processed and incubated as in (C) with the following conditions: water, DMSO (amount equivalent to a concentration of 7 $\alpha$ ,25-OHC 3,000 nM), 7 $\alpha$ ,25-OHC 300 nM, 7 $\alpha$ ,25-OHC 3,000 nM, or NIBR189 25 nM, with lysis buffer as positive control. The lactate dehydrogenase (LDH) release was measured by spectrophotometry.

Statistics using two-way ANOVA with a Tukey's post hoc analysis, with a  $p$  value  $\leq 0.05$  considered significant (\*). Error bars represent median in (A) and SEM in (B).

**Table 1. Patient Characteristics**

	Gender	Mean Age ( $\pm$ SEM)	n	Mean EDSS at T0 ( $\pm$ SEM)	Mean EDSS during T9–T12 ( $\pm$ SEM)	Disease Mean Duration (Years) at Blood Draw ( $\pm$ SEM)	Previous DMT
Healthy donors	female	37.42 (3.40)	12	–	–	–	–
	male	34.50 (3.75)	4	–	–	–	–
RRMS patients	female	35.22 (2.06)	11	2.14 (0.19)	–	2.57 (1.32)	11 no treatment
	male	34.60 (3.61)	4	1.88 (0.24)	–	1.85 (1.14)	3 no treatment 1 natalizumab (stopped 5 months before sampling)
NTZ patients	female	33.72 (3.32)	10	2.75 (0.45)	2.45 (0.43)	6.40 (1.94)	6 interferon-beta 2 glatiramer acetate 1 fingolimod (stopped 2 months before sampling) 1 untreated
	male	39.00 (0.00)	1	3.00 (0.00)	3.00 (0.00)	7.00 (0.00)	no treatment (interferon-beta stopped 12 months before sampling)

Clinical features from patients included in the study. Age and disease duration are in years. RRMS, relapsing-remitting multiple sclerosis; NTZ, natalizumab treated; DMT, disease-modifying treatment; T, time (months); EDSS, expanded disability status scale.

T0 and at T9–T12. At both time points, EB12 inhibition was equally efficient in memory CD4<sup>+</sup> T cells (from a mean of 11.8 ( $\pm$ 4) to 1.8 ( $\pm$ 0.5) at T0 and 18.2 ( $\pm$ 8) to 1.6 ( $\pm$ 0.7) at T9–T12) despite the increase in migration toward 7 $\alpha$ ,25-OHC at T9–T12 (Figure 4C).

We next asked whether EB12 expression was correlated to migration toward 7 $\alpha$ ,25-OHC. As seen in RRMS samples, there was a positive correlation at NTZ T0 and at NTZ T9–T12 in CD4<sup>+</sup> T cells (Figure 4D). However, no difference in correlation was observed between the two time points.

We then determined whether NTZ could increase EB12 expression when added directly on memory CD4<sup>+</sup> T cells in vitro. PBMCs were cultured in vitro in the presence or not of physiologic concentrations of NTZ (100  $\mu$ g/mL, corresponding to the maximum serum concentration observed in humans) (Kivisäkk et al., 2009). The sole addition of NTZ on memory CD4<sup>+</sup> T cells in vitro was not able to upregulate EB12 (Figure S3A). However, 7 $\alpha$ ,25-OHC exposition decreased EB12 expression levels when added in parallel, thus confirming that modulation of human EB12 at the protein level was feasible in vitro (Figure S3B).

### EB12 and CD11a Expressions Are Negatively Correlated in Memory CD4<sup>+</sup> T Cells during Natalizumab Treatment

To compare the evolution of EB12 expression to another marker known to be affected by NTZ, we decided to assess the expression of the  $\alpha$  subunit of LFA-1, CD11a, which was shown to decrease in T cells upon NTZ treatment (Jilek et al., 2014). In our patients, CD11a fluorescence was predominant in memory subsets of CD4<sup>+</sup> T cells, and its expression was significantly diminished at T9–T12 compared to T0 in all CD4<sup>+</sup> and CD8<sup>+</sup> T cell subsets (Figure 5A) but not in B cells. We next wondered whether EB12 and CD11a were co-expressed on memory CD4<sup>+</sup> T cells. Most EB12-positive cells co-expressed CD11a (Figure 5B). Under NTZ treatment, the percentage of cells co-expressing EB12 with CD11a was not altered; however, the percentage of memory CD4<sup>+</sup> T cells that were EB12 single positive

increased significantly while the percentage of cells single positive for CD11a decreased significantly (Figure 5B, plots and graphic). Those results suggest a possible interaction between those two surface receptors.

### DISCUSSION

Oxysterols and EB12 have received growing attention in the field of immunology, with works highlighting an important role for EB12 in immune cell migration. However, these studies are mainly limited to animal models (Chalmin et al., 2015; Hannedouche et al., 2011; Kelly et al., 2011; Liu et al., 2011; Pereira et al., 2009; Suan et al., 2015), while in human and particularly in a disease setting, such as MS, the relevance of EB12 expression and function remains a critical question to potentially translate research findings from the bench side to the patient.

We here report that EB12 is functional and differentially expressed at the surface of human lymphocytes, with a strong predominance for CD4<sup>+</sup> T and B cell memory subsets. These observations obtained at the protein level are in line with previous mRNA data (Hannedouche et al., 2011) showing predominant EB12 expression in human memory subsets of B cells and CD4<sup>+</sup> and CD8<sup>+</sup> T cells, and they corroborate murine data showing a higher EB12 expression in mature B cells compared to naive correlates (Pereira et al., 2009). Curiously, despite similar EB12 expression levels between memory CD4<sup>+</sup> T cells and B cells, CD4<sup>+</sup> T cells migrate twice as much as their B cell counterparts. Technically, this could be secondary to differences between B and CD4<sup>+</sup> T cells about the optimal oxysterol concentrations for migration in our assay or to a higher sensitivity of B cells to the thawing process. However, previous murine data show a similar migration between B220<sup>+</sup> B cells and CD4<sup>+</sup> T cells (Liu et al., 2011). Therefore, possible differences between human B and CD4<sup>+</sup> T cell migration patterns cannot be dismissed, and they could be secondary to differences in EB12 signaling or to distinct interactions with other adhesion or activation molecules. No positive correlation between the migration

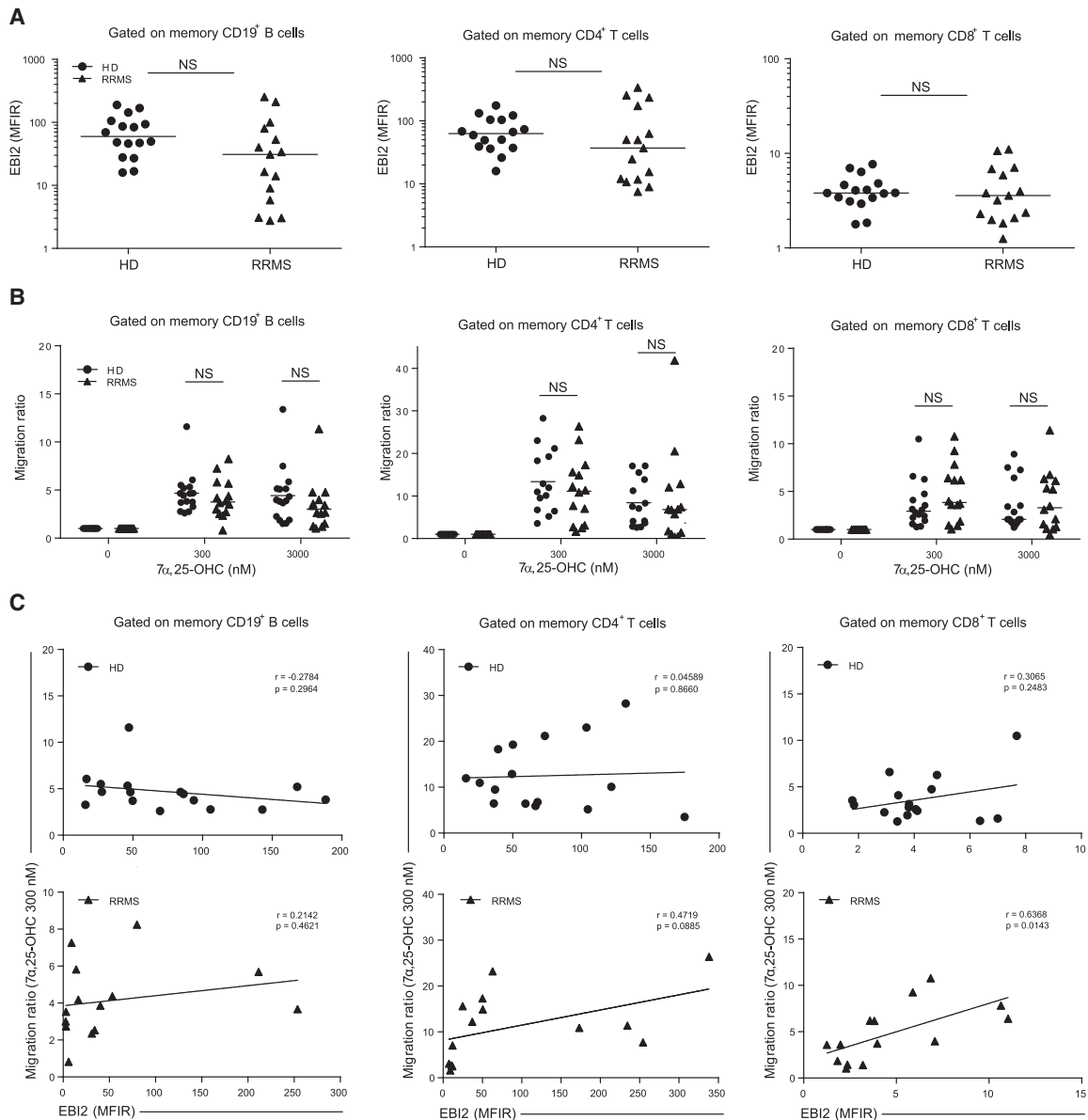


**Figure 3. EB12 Expression and Migration Rate in Lymphocytes from Untreated RRMS Patients**

(A) EB12 MFIRs in memory B and CD4<sup>+</sup> T cells in HDs (n = 16) and RRMS patients (n = 15).

(B) Migration rates toward 7α,25-OHC (0, 300, and 3,000 nM) in memory subsets of CD19<sup>+</sup> B cells, CD4<sup>+</sup> T cells, and CD8<sup>+</sup> T cells from HDs (n = 16) and RRMS patients (n = 14).

(C) Correlation of EB12 expression (MFIR) and migration toward 7α,25-OHC 300 nM in memory CD19<sup>+</sup> B cells, CD4<sup>+</sup> cells and CD8<sup>+</sup> T cells from HDs (n = 16, upper panels) or untreated RRMS patients (n = 14, lower panels).

Statistical analysis used two-way ANOVA with a Tukey's post hoc analysis or unpaired t test, linear regression, and Pearson correlation test, with a p value ≤ 0.05 considered significant (\*). Error bars represent median.

rate toward 7α,25-OHC and EB12 expression was observed in different subsets of lymphocytes obtained from HDs. On the contrary, a positive correlation between EB12 expression and migration toward 7α,25-OHC was observed in RRMS patients (both untreated or under DMTs). This is particularly relevant for CD4<sup>+</sup> and CD8<sup>+</sup> memory T cells but not for CD19<sup>+</sup> B cells. Those correlation differences between HDs and RRMS patients could

indicate that EB12 signaling or interactions with other adhesion molecules differ during autoimmunity.

In addition, the similar levels of EB12 expression in untreated RRMS patients might not exclude changes in EB12 expression and/or function in more severe disease states or at precise moments during the disease evolution. Because it was described that upon certain stimuli (i.e., lipopolysaccharides [LPS]

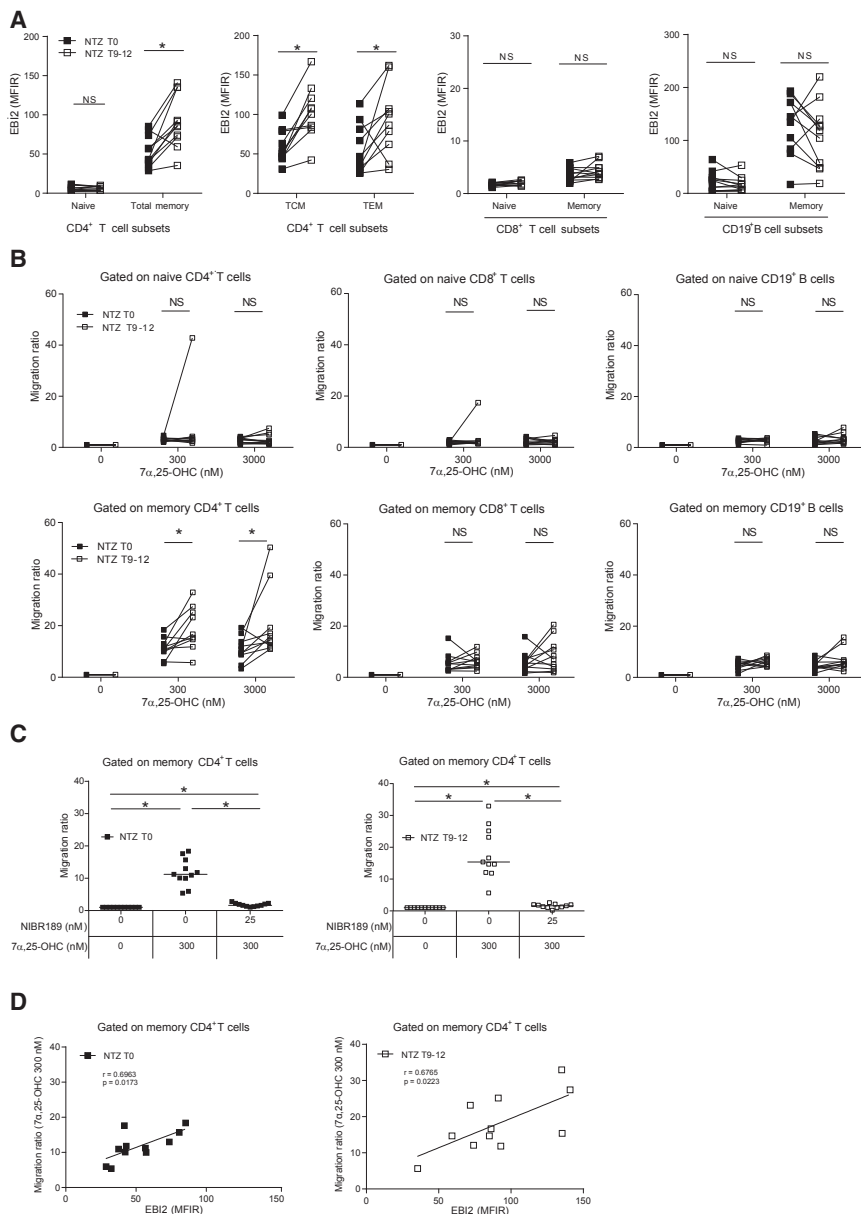


**Figure 4. Memory CD4<sup>+</sup> T Cells from NTZ-Treated Patients Show Increased EB12 Expression and Migration Response to 7 $\alpha$ ,25-OHC**

Cryopreserved PBMCs from RRMS patients before (T0) or after 9–12 months of NTZ treatment (T9–T12) were analyzed by flow cytometry for EB12 expression, and migration was assessed by transwell assay.

(A) EB12 expression shown as MFIRs in CD4<sup>+</sup> T cell, CD8<sup>+</sup> T cell, and CD19<sup>+</sup> B cell naive and memory subsets (n = 11), including TCM and TEM (n = 10).

(B) Migration in response to 7 $\alpha$ ,25-OHC (0, 300, and 3,000 nM) in naive (upper panels) versus memory (lower panels) subsets of CD4<sup>+</sup> and CD8<sup>+</sup> T cells, as well as CD19<sup>+</sup> B cells.

(C) Migration in response to 7 $\alpha$ ,25-OHC (0 and 300 nM) of memory CD4<sup>+</sup> T cells from RRMS patients before and after NTZ treatment onset without or with EB12 inhibition by NIBR189 (n = 11).

(D) Correlation of EB12 expression (MFIR) with migration toward 7 $\alpha$ ,25-OHC 300 nM in NTZ T0 (left panel) and NTZ T9–T12 (right panel) (n = 11). Statistical analysis using two-way ANOVA with a Tukey’s post hoc analysis or paired t test, linear regression, and Pearson correlation test, with a p value  $\leq$  0.05 considered significant (\*). Error bars represent median. See also Figures S2 and S3 and Table S1.

normal or pathologic conditions or participate in CD4<sup>+</sup> T cell homing to secondary lymphoid organs. Regarding the latter hypothesis, given that EB12 expression in peripheral blood naive CD4<sup>+</sup> T cells is very low and that, in the memory subsets, we did not see any difference in expression between central and effector memory T cells, it is unlikely that EB12 might specifically participate in this process. However, the observation by Preuss et al. (2014) that EB12 RNA transcripts are maximal in human primary monocytes and upregulated in M0 macrophages upon LPS challenge brings arguments for a potential role of EB12 for site-specific migration of immune cells during inflammatory settings. Future investigations are required to clarify this point.

We further assessed EB12 expression in RRMS patients before and during NTZ treatment. A significant increase of EB12 expression was observed in memory CD4<sup>+</sup> T cell subpopulations, but not in CD8<sup>+</sup> T cell or in CD19<sup>+</sup> B cell subsets of patients undergoing NTZ treatment, with a parallel gain in the migration rate toward 7 $\alpha$ ,25-OHC compared to before treatment onset. Those changes are likely specific to NTZ, because other DMTs do not elicit such a response and EB12 expression was not correlated with disease severity or duration. The effects of NTZ treatment on EB12 could be either direct or indirect. We favor the second postulate, because the sole addition of NTZ on PBMCs was

challenge), human macrophages upregulated EB12 RNA expression in only 2 hr with return to basal level after 4 hr (Preuss et al., 2014), we can hypothesize that EB12 expression and/or function may vary in a transient and possibly highly dynamic course in lymphocytes depending on the disease evolution. Accurate time points according to the relapses may be necessary to highlight such changes.

EB12 is important for the migration of myeloid and lymphoid cells in steady-state and inflammatory conditions (Chalmin et al., 2015; Chiang et al., 2013; Gatto et al., 2013; Hannedouche et al., 2011; Kelly et al., 2011; Liu et al., 2011; Pereira et al., 2009; Preuss et al., 2014; Rutkowska et al., 2015; Suan et al., 2015; Yi et al., 2012). We can therefore hypothesize that EB12 may also play a role in organ-specific migration of memory cells during

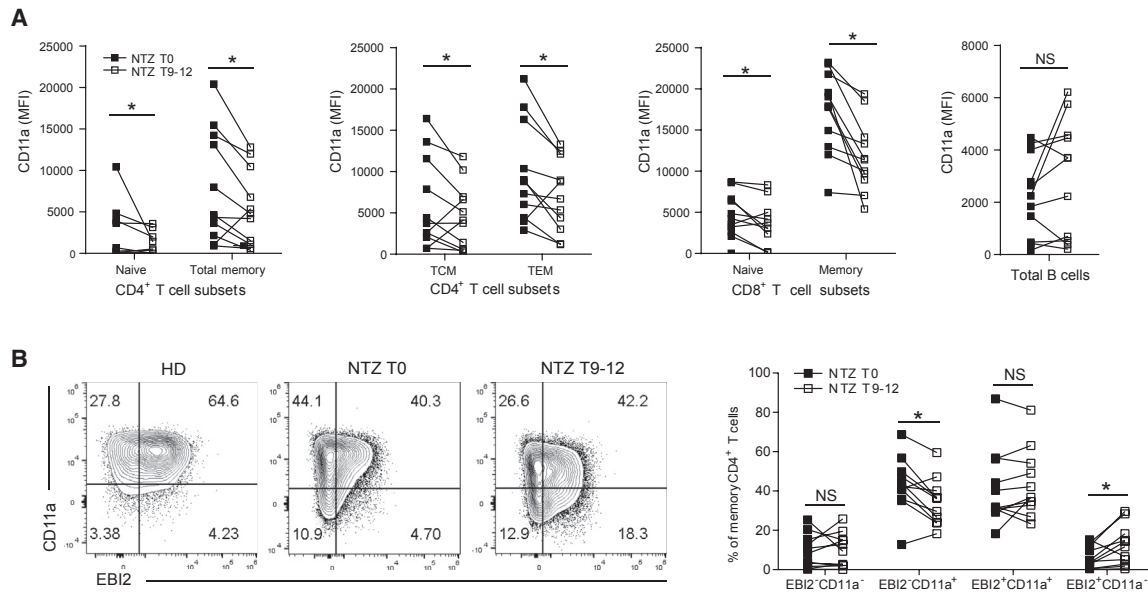


**Figure 5. NTZ-Treated Patients Depict Decreased CD11a Expression in T Cell Subsets**

PBMCs from HDs and NTZ patients were analyzed by flow cytometry.

(A) CD11a expression in NTZ T0 and T9–T12 shown as mean fluorescence intensity in CD4<sup>+</sup> and CD8<sup>+</sup> T cell naive versus memory subsets and in total B cells (n = 11).

(B) Percentages of memory CD4<sup>+</sup> T cells expressing EBI2 and/or CD11a shown on representative dot plots (left panels) and on a graphic (right panel) (n = 11). Statistics using paired t test, linear regression, and Pearson correlation test.

not sufficient to induce EBI2 at the protein level. This is reminiscent of the effect of NTZ on lymphocyte proliferation described previously, in which the increased number of lymphocytes observed in the blood of patients under NTZ treatment did not correlate with an increase in lymphocyte proliferation obtained from PBMCs when NTZ was added in vitro (Kivisäkk et al., 2009). As another option, EBI2 upregulation in memory CD4<sup>+</sup> T cells could be driven in a different compartment than blood (such as in the bone marrow or in secondary lymphoid organs), potentially requiring interactions in vivo that are still to be explored. Besides, the increase in EBI2 expression is mirrored by a decrease in CD11a (LFA-1) expression. On this point, the upregulation of one receptor can be potentially related to the downregulation of another through imbalances in recruitment of common adaptor molecules. In addition, EBI2 is mainly co-expressed on memory CD4<sup>+</sup> T cells with LFA-1 in untreated RRMS patients, while under NTZ treatment, a significant subset of CD4<sup>+</sup> T cells were EBI2<sup>+</sup> but LFA-1<sup>-</sup>. These changes in receptor co-expression might affect the migration of CD4<sup>+</sup> T cells and the disease evolution in particular under NTZ treatment. Further investigations are needed to better understand the interplay among integrins, chemokine receptors, and EBI2 during MS and in particular under DMTs such as NTZ.

NTZ treatment is associated with an increased risk of progressive multifocal leukoencephalopathy (PML), due to John Cunningham (JC) virus reactivation or infection (McGuigan et al., 2016). Because T cells are important for brain immune surveillance (Dubois et al., 2015), an increase in EBI2 detection and function in the context of NTZ administration could be a compensatory reaction to favor CD4<sup>+</sup> T cell homing to the brain and/or

cerebrospinal fluid (CSF). It would be interesting to test whether a lack of EBI2 upregulation may affect PML development. However, it is not clear whether this increase in EBI2 expression under NTZ plays a role in the “rebound” effect of disease burden, which often follows NTZ arrest. Brain inflammatory infiltrates in patients with rebound effect are mainly constituted of CD8<sup>+</sup> T cells with CD4<sup>+</sup> T cells concomitantly enriched in CSF, while during NTZ treatment, CD4<sup>+</sup> T cells are dramatically diminished in CSF, suggesting an important role for the latter cells in this compartment (Larochelle et al., 2016; Stüve et al., 2006). EBI2 might be involved in the localization of these cells; therefore, its expression changes under NTZ could have potential effects on disease activity. Previous works have highlighted significant participation for EBI2 in B and Tfh cells to regulate B cell maturation and T-dependent antibody response, with simultaneous modulation of the receptor expression to changes in 7 $\alpha$ ,25-OHC production by surrounding cells (Hannedouche et al., 2011; Li et al., 2016; Suan et al., 2015; Yi et al., 2012). Therefore, we can hypothesize that there may be EBI2-oxysterol cross-talk between memory CD4<sup>+</sup> T cells and the blood brain barrier (BBB). This interaction could be affected by NTZ treatment; thus, T cell migration may be affected. It remains to be unraveled whether an oxysterol gradient can be generated by the BBB, potentially involving 7 $\alpha$ ,25-OHC production by the endothelium, pericytes, or perivascular space macrophages. The 7 $\alpha$ ,25-OHC synthesizing enzymes are expressed in blood endothelial cells of lymph nodes (Yi et al., 2012), in macrophages (Preuss et al., 2014), and in astrocytes (Rutkowska et al., 2016), reinforcing a potential role for the BBB in oxysterol synthesis. In the setting of the rebound effect, further investigations are required to better

understand the participation of EB12 in the migration of pathogenic CD4<sup>+</sup> T cells beyond the BBB. Because an inhibitor is available with NIBR189, which efficiently blocks EB12 in human lymphocytes and in NTZ-treated patients, this could open alternative therapeutic opportunities.

In conclusion, our work brings additional elements into the comprehension of the role of EB12 in human, particularly during MS and NTZ treatment. Even if many questions are still open, these results offer a promising field for future studies and innovative perspectives for therapeutic approaches.

## EXPERIMENTAL PROCEDURES

### Patients

We enrolled 14 healthy donors from Geneva University Hospital Transfusion Center, two healthy volunteers, 14 patients with RRMS with no DMT undergoing a mild relapse which did not necessitate corticosteroid administration, and 11 patients treated with natalizumab (300 mg intravenously [i.v.] monthly) from the Lausanne University Hospital (Table 1). The ethical commissions from the Lausanne University Hospital accepted this study, and all RRMS patients gave their written informed consent, according to review board guidelines. At the time of enrollment, the diagnosis of MS was made using the revised McDonald's criteria 2010 (Polman et al., 2011). Patients were considered relapsing if a relapse had started within 4 weeks of the blood sample draw. For natalizumab and dimethyl fumarate-treated patients, blood samples were drawn just before the first administration and then after 9–12 months.

### PBMC Extraction, Cryopreservation, and Thawing

All blood sampling used Sarstedt Monovette EDTA K3 tubes. PBMCs were extracted by gradient centrifugation using either Ficoll-Paque Plus (GE Healthcare) or Lymphoprep (STEMCELL Technologies). The leukocyte ring was removed and washed in RPMI (Sigma) completed with penicillin, streptomycin, and glutamine (PSG) (all from Sigma). Viable cells were counted using trypan blue (Sigma) resuspended in heat-inactivated fetal calf serum (FCS) 90% (Eurobio) with 10% DMSO (Sigma) at 10<sup>7</sup> cells/mL, and transferred into cryotubes. Tubes were then frozen and kept in liquid nitrogen. Cells were thawed and resuspended at 10<sup>6</sup> cells/mL in the RPMI-PSG-10% FCS and plated in a 96-well round bottom plate for overnight resting at 37°C in a cell incubator.

### Flow Cytometry Analysis

PBMCs (prepared as described earlier) from each patient were separated to be either directly stained for viability with Live/Dead Fixable Yellow Dead Cell Stain Kits (Invitrogen) and surface markers or tested for migration assay on the same day. The cells were first washed in PBS and then stained with Live/Dead Fixable Dead Cell Stain according to the manufacturer's instructions for 30 min in dark on ice, washed again in PBS, and resuspended in antibodies diluted in PBS-BSA-1%. After 15 min incubation at room temperature (RT) in dark, cells were washed twice in PBS-BSA-1%, and resuspended in Phosflow fixation buffer (Becton Dickinson [BD]) for 15 min at RT in dark. Cells were then washed twice in PBS-BSA-1% and resuspended in this buffer for flow cytometry analysis. The following antibodies were purchased from eBioscience: CD4 (RPA-T4), CD45RA (HI100), IgG2a isotype (eBM2a), and CD19 (HIB19). Antibodies were also purchased from BioLegend: CD8 (SK1), CD4 (SK3), CD45RA (HI100), CD56 (HCD56), CD27 (M-T271), and CD19 (HIB19). The following antibodies were purchased from BD: CD197 (CCR7) (150503), CD11a (HI111), and CD3 (SK7). The fluorochrome-labeled EB12 antibody (57C9B5C9) was provided by Andreas Sailer of Novartis. All patient samples were analyzed with a Gallios 3 cytometer (Beckman Coulter). To compensate for laser senescence and improve comparability of the fluorescences obtained along the study, for each EB12 phenotypization experiment, voltages were standardized using Rainbow Calibration particles, eight peaks (BioLegend), with tolerance of a 5% error margin in each detection canal used. All flow cytometry data were analyzed using FlowJo software (v.X, Tree Star).

### In Vitro Migration Assay

After thawing, PBMCs were washed in a medium composed of DMEM (Gibco) complemented with minimal essential medium (MEM) vitamins (100×), MEM non-essential amino acid solution (100×), sodium pyruvate 1.5 mM, folic acid 14 mM, L-asparagine 0.3 mM, L-arginine 0.7 mM, L-glutamine 2 mM, penicillin-streptomycin 100 U/mL, BSA 1%, β-mercaptoethanol 14.3 mM (all from Sigma-Aldrich) and were resuspended in this medium at 1.5 million cells/mL. The indicated dilutions of DMSO (Sigma), 7α,25-OHC (provided by Novartis, reconstituted in DMSO at 10 mM), CXCL12 (Peprotech, reconstituted in PBS and BSA 0.1% at 100 μg/mL), and NIBR189 (reconstituted in DMSO at 10 mM) were prepared using the same medium. The 240 μL of 7α,25-OHC, CXCL12, or medium only were added to the lower chamber of a 96-well transwell plate (Corning, 3387); 75 μL of cells, with or without NIBR189, were then transferred into the top chamber of the transwell. The plate was then incubated for 3 hr at 37°C in a cell incubator. The cells that migrated into the lower chamber were stained for surface markers and quantified by flow cytometry using fluorescent beads (Flow-Count Fluorospheres, Beckman Coulter) and a Gallios 3 cytometer (Beckman Coulter). A pre-defined number of beads were added directly to cells for a total initial volume of 200 μL. The number of beads finally counted by the cytometer was then used to calculate the effective volume analyzed in each tube so that the accurate number of cells per microliter in each tube could be calculated.

### Cytotoxicity Assay and Cell Viability

7α,25-OHC and NIBR189 cell toxicity was assessed using the Pierce lactate dehydrogenase (LDH) cytotoxicity assay kit (Thermo Scientific). Human PBMCs were thawed and plated in RPMI-PSG-10% FCS for overnight resting. Then, cells were washed, counted, and resuspended in the medium used for migration assay (described earlier). After plating at 1.5 million cells/mL in a 96-well plate with 10 μL water, DMSO (amount equivalent to a concentration of 7α,25-OHC 3,000 nM), 7α,25-OHC 300 nM, 7α,25-OHC 3,000 nM, or NIBR189 25 nM, they were incubated for 3 hr in a cell incubator at 37°C. Lysis buffer (10×) furnished by the manufacturer was used as positive control, water was used as negative control, and the percentage of LDH release secondary to cell lysis was measured by spectrophotometry. To test for cell viability in the presence of NIBR189, PBMCs were thawed, rested, and incubated 3 hr at 37°C with NIBR189 at the concentration of 25 nM in the same way as for the cytotoxicity assay. Then, cells were stained with Live/Dead Fixable Dead Cell Stain as described in the Flow Cytometry Analysis section and analyzed with a Gallios 3 cytometer (Beckman Coulter).

### Statistical Analysis

Statistical analysis was performed with GraphPad Prism software v.7. The differences in the immune populations were analyzed with two-way ANOVA associated to Tukey's multiple comparison post hoc analysis or unpaired t test when appropriate, and paired t test was used to analyze the difference between time points. A *p* value ≤ 0.05 was considered significant. For correlation analysis, linear regression test and Pearson correlation test were used.

## SUPPLEMENTAL INFORMATION

Supplemental Information includes three figures and one table and can be found with this article online at <http://dx.doi.org/10.1016/j.celrep.2016.12.006>.

## AUTHOR CONTRIBUTIONS

A.S.C., research conception and design, acquisition and interpretation of data, and manuscript preparation. A.M., patient selection and technical and scientific assistance. A.W.S., scientific and logistical assistance. M.S., MS patient cohort management. J.D.S., scientific, academic, and logistical assistance. R.D.P., scientific assistance and providing of patient samples. C.P., research conception and design, interpretation of data, and manuscript preparation.

## ACKNOWLEDGMENTS

We acknowledge Géraldine Le Goff and Mathieu Canales for blood sampling, Cécile Gameiro and Jean-Pierre Aubry for flow cytometry technical assistance, Giuseppe Pantaleo for support, and Britta Engelhardt, Gisella Puga-Young, Nicolo Brembilla, and Matthieu Perreau for scientific discussions. This work was supported by the Swiss National Science Foundation (PP00P3\_157476), the Swiss Multiple Sclerosis Society, and the Ernst and Lucie Schmidheiny Foundation. C.P. holds stipendiary professorships of the Swiss National Science Foundation (PP00P3\_157476). A.S.C. is supported by the Hirsch Foundation and the Clinical Research Center (Geneva University Hospitals). A.W.S. is employee of Novartis Pharma and holds stock and stock options in his company.

Received: July 12, 2016

Revised: November 6, 2016

Accepted: November 30, 2016

Published: January 3, 2017

## REFERENCES

- Bauman, D.R., Bitmansour, A.D., McDonald, J.G., Thompson, B.M., Liang, G., and Russell, D.W. (2009). 25-Hydroxycholesterol secreted by macrophages in response to Toll-like receptor activation suppresses immunoglobulin A production. *Proc. Natl. Acad. Sci. USA* 106, 16764–16769.
- Börnsen, L., Christensen, J.R., Ratzner, R., Oturai, A.B., Sørensen, P.S., Søndergaard, H.B., and Sellebjerg, F. (2012). Effect of natalizumab on circulating CD4+ T-cells in multiple sclerosis. *PLoS ONE* 7, e47578.
- Chalmin, F., Rochemont, V., Lippens, C., Clottu, A., Sailer, A.W., Merkler, D., Hugues, S., and Pot, C. (2015). Oxysterols regulate encephalitogenic CD4(+) T cell trafficking during central nervous system autoimmunity. *J. Autoimmun.* 56, 45–55.
- Chiang, E.Y., Johnston, R.J., and Grogan, J.L. (2013). EBI2 is a negative regulator of type I interferons in plasmacytoid and myeloid dendritic cells. *PLoS ONE* 8, e83457.
- Compston, A., and Coles, A. (2002). Multiple sclerosis. *Lancet* 359, 1221–1231.
- Dubois, E., Ruschil, C., and Bischof, F. (2015). Low frequencies of central memory CD4 T cells in progressive multifocal leukoencephalopathy. *Neurol. Neuroimmunol. Neuroinflamm.* 2, e177.
- Eibinger, G., Fauler, G., Bernhart, E., Frank, S., Hammer, A., Wintersperger, A., Eder, H., Heinemann, A., Mischel, P.S., Malle, E., and Sattler, W. (2013). On the role of 25-hydroxycholesterol synthesis by glioblastoma cell lines. Implications for chemotactic monocyte recruitment. *Exp. Cell Res.* 319, 1828–1838.
- Engelhardt, B., and Kappos, L. (2008). Natalizumab: targeting alpha4-integrins in multiple sclerosis. *Neurodegener. Dis.* 5, 16–22.
- Engelhardt, B., and Ransohoff, R.M. (2012). Capture, crawl, cross: the T cell code to breach the blood-brain barriers. *Trends Immunol.* 33, 579–589.
- Gatto, D., Paus, D., Basten, A., Mackay, C.R., and Brink, R. (2009). Guidance of B cells by the orphan G protein-coupled receptor EBI2 shapes humoral immune responses. *Immunity* 31, 259–269.
- Gatto, D., Wood, K., Caminschi, I., Murphy-Durland, D., Schofield, P., Christ, D., Karupiah, G., and Brink, R. (2013). The chemotactic receptor EBI2 regulates the homeostasis, localization and immunological function of splenic dendritic cells. *Nat. Immunol.* 14, 446–453.
- Gessier, F., Preuss, I., Yin, H., Rosenkilde, M.M., Laurent, S., Endres, R., Chen, Y.A., Marsilje, T.H., Seuwen, K., Nguyen, D.G., and Sailer, A.W. (2014). Identification and characterization of small molecule modulators of the Epstein-Barr virus-induced gene 2 (EBI2) receptor. *J. Med. Chem.* 57, 3358–3368.
- Hannedouche, S., Zhang, J., Yi, T., Shen, W., Nguyen, D., Pereira, J.P., Guerini, D., Baumgarten, B.U., Roggo, S., Wen, B., et al. (2011). Oxysterols direct immune cell migration via EBI2. *Nature* 475, 524–527.
- Jilek, S., Mathias, A., Canales, M., Lysandropoulos, A., Pantaleo, G., Schluep, M., and Du Pasquier, R.A. (2014). Natalizumab treatment alters the expression of T-cell trafficking marker LFA-1  $\alpha$ -chain (CD11a) in MS patients. *Mult. Scler.* 20, 837–842.
- Kelly, L.M., Pereira, J.P., Yi, T., Xu, Y., and Cyster, J.G. (2011). EBI2 guides serial movements of activated B cells and ligand activity is detectable in lymphoid and nonlymphoid tissues. *J. Immunol.* 187, 3026–3032.
- Kivisäkk, P., Healy, B.C., Viglietta, V., Quintana, F.J., Hootstein, M.A., Weiner, H.L., and Khoury, S.J. (2009). Natalizumab treatment is associated with peripheral sequestration of proinflammatory T cells. *Neurology* 72, 1922–1930.
- Larochelle, C., Metz, I., Lécuyer, M.A., Terouz, S., Roger, M., Arbour, N., Brück, W., and Prat, A. (2016). Immunological and pathological characterization of fatal rebound MS activity following natalizumab withdrawal. *Mult. Scler.* 1352458516641775.
- Li, J., Lu, E., Yi, T., and Cyster, J.G. (2016). EBI2 augments Tfh cell fate by promoting interaction with IL-2-quenching dendritic cells. *Nature* 533, 110–114.
- Liu, C., Yang, X.V., Wu, J., Kuei, C., Mani, N.S., Zhang, L., Yu, J., Sutton, S.W., Qin, N., Banie, H., et al. (2011). Oxysterols direct B-cell migration through EBI2. *Nature* 475, 519–523.
- Liu, K.K., and Dorovini-Zis, K. (2009). Regulation of CXCL12 and CXCR4 expression by human brain endothelial cells and their role in CD4+ and CD8+ T cell adhesion and transendothelial migration. *J. Neuroimmunol.* 215, 49–64.
- McGuigan, C., Craner, M., Guadagno, J., Kapoor, R., Mazibrada, G., Molyneux, P., Nicholas, R., Palace, J., Pearson, O.R., Rog, D., and Young, C.A. (2016). Stratification and monitoring of natalizumab-associated progressive multifocal leukoencephalopathy risk: recommendations from an expert group. *J. Neurol. Neurosurg. Psychiatry* 87, 117–125.
- Mehling, M., Brinkmann, V., Antel, J., Bar-Or, A., Goebels, N., Vedrine, C., Kristofic, C., Kuhle, J., Lindberg, R.L., and Kappos, L. (2008). FTY720 therapy exerts differential effects on T cell subsets in multiple sclerosis. *Neurology* 71, 1261–1267.
- Nevius, E., Pinho, F., Dhodapkar, M., Jin, H., Nadrah, K., Horowitz, M.C., Kikuta, J., Ishii, M., and Pereira, J.P. (2015). Oxysterols and EBI2 promote osteoclast precursor migration to bone surfaces and regulate bone mass homeostasis. *J. Exp. Med.* 212, 1931–1946.
- Pereira, J.P., Kelly, L.M., Xu, Y., and Cyster, J.G. (2009). EBI2 mediates B cell segregation between the outer and centre follicle. *Nature* 460, 1122–1126.
- Polman, C.H., O'Connor, P.W., Havrdova, E., Hutchinson, M., Kappos, L., Miller, D.H., Phillips, J.T., Lublin, F.D., Giovannoni, G., Wajgt, A., et al.; AFFIRM Investigators (2006). A randomized, placebo-controlled trial of natalizumab for relapsing multiple sclerosis. *N. Engl. J. Med.* 354, 899–910.
- Polman, C.H., Reingold, S.C., Banwell, B., Clanet, M., Cohen, J.A., Filippi, M., Fujihara, K., Havrdova, E., Hutchinson, M., Kappos, L., et al. (2011). Diagnostic criteria for multiple sclerosis: 2010 revisions to the McDonald criteria. *Ann. Neurol.* 69, 292–302.
- Preuss, I., Ludwig, M.G., Baumgarten, B., Bassilana, F., Gessier, F., Seuwen, K., and Sailer, A.W. (2014). Transcriptional regulation and functional characterization of the oxysterol/EBI2 system in primary human macrophages. *Biochem. Biophys. Res. Commun.* 446, 663–668.
- Rutkowska, A., Preuss, I., Gessier, F., Sailer, A.W., and Dev, K.K. (2015). EBI2 regulates intracellular signaling and migration in human astrocyte. *Glia* 63, 341–351.
- Rutkowska, A., O'Sullivan, S.A., Christen, I., Zhang, J., Sailer, A.W., and Dev, K.K. (2016). The EBI2 signalling pathway plays a role in cellular crosstalk between astrocytes and macrophages. *Sci. Rep.* 6, 25520.
- Sallusto, F., Lenig, D., Förster, R., Lipp, M., and Lanzavecchia, A. (1999). Two subsets of memory T lymphocytes with distinct homing potentials and effector functions. *Nature* 401, 708–712.
- Stüve, O., Marra, C.M., Bar-Or, A., Niino, M., Cravens, P.D., Cepok, S., Frohman, E.M., Phillips, J.T., Arendt, G., Jerome, K.R., et al. (2006). Altered CD4+/CD8+ T-cell ratios in cerebrospinal fluid of natalizumab-treated patients with multiple sclerosis. *Arch. Neurol.* 63, 1383–1387.

Suan, D., Nguyen, A., Moran, I., Bourne, K., Hermes, J.R., Arshi, M., Hampton, H.R., Tomura, M., Miwa, Y., Kelleher, A.D., et al. (2015). T follicular helper cells have distinct modes of migration and molecular signatures in naive and memory immune responses. *Immunity* 42, 704–718.

Yi, T., Wang, X., Kelly, L.M., An, J., Xu, Y., Sailer, A.W., Gustafsson, J.A., Russell, D.W., and Cyster, J.G. (2012). Oxysterol gradient generation by lymphoid stromal cells guides activated B cell movement during humoral responses. *Immunity* 37, 535–548.